

Characterization of $(\text{La}_{0.9}\text{Sr}_{0.1})_{0.95}\text{Cr}_{0.85}\text{Mg}_{0.1}\text{Ni}_{0.05}\text{O}_3$ Perovskite Ceramics for a Perovskite Related Membrane Reactor

Rachel Rosten¹, Matthew Swanson¹, Jakob Kuebler², Jayanta Kapat³, and Nina Orlovskaya³

¹Department of Materials Science and Engineering, Michigan Technological University, Houghton, MI, 49931

²EMPA - Material Science & Technology, Duebendorf, Switzerland

³Department of Mechanical, Materials, and Aerospace Engineering, University of Central Florida, Orlando, FL, 32816

ABSTRACT

In this research we investigated the sintering behavior of $(\text{La}_{0.9}\text{Sr}_{0.1})_{0.95}\text{Cr}_{0.85}\text{Mg}_{0.1}\text{Ni}_{0.05}\text{O}_3$ perovskite which is a potential candidate material for enhancing the oxidation reactions in oxygen separation and syngas production. It was found that solid state sintering occurs as a single step event and it was possible to produce gas tight ceramics after using cold isostatic pressing followed by sintering at 1700°C in air. Grain size, porosity, and lattice parameter measurements of the pressureless sintered ceramics were performed as a function of sintering temperature. A small amount of secondary phases was also detected by XRD and EDS analysis.

INTRODUCTION

Perovskite ceramic reactors are a promising new way to generate pure oxygen. In such reactors dense, gas tight ceramic membranes simultaneously conductive to both oxygen ions and electrons provide high oxygen fluxes. When a gradient of oxygen chemical potential is imposed across these dense membranes at high temperatures, oxygen ions are transported from the high- to low-partial-pressure side and released downstream of the oxygen fluxes.

La-Cr-O based perovskites are highly promising for use in perovskite membranes to enhance the oxidation reactions on the fuel side. They might perform extremely well as a catalytically active surface layer deposited on the fuel side of the membrane, especially if Cr ions can be substituted with such cations as Ni, which are well known to enhance the fuel reforming or oxidation processes. Yet La-Cr-O based perovskites are also known to be very difficult to sinter to full density. Different sintering strategies have been developed, such as addition of sintering aids [1], substitution of chromium and lanthanum by other cations [1, 2, 3], sintering in a reducing atmosphere [4], and using chromium deficient nonstoichiometric compositions [5, 6].

The goal of this research was to characterize the sintering behavior and structural evolution of the $(\text{La}_{0.9}\text{Sr}_{0.1})_{0.95}\text{Cr}_{0.85}\text{Mg}_{0.1}\text{Ni}_{0.05}\text{O}_3$ (LSCMN) perovskite and, therefore, the results of the perovskite sintering behavior, phase, and microstructural development are presented as a function of sintering temperature. Different analysis techniques have been employed including the liquid immersion technique for density measurement, sintering shrinkage dilatometry, powder X-ray diffraction (XRD), and field emission scanning electron microscopy (FESEM) coupled with energy dispersive X-ray spectroscopy (EDS) that allowed us to characterize the structure of the LSCMN perovskite.

EXPERIMENT

The LSCMN powder was produced by Praxair Specialty Ceramics, USA. The sintering behavior of LSCMN was studied by a Bahr Dil802 dilatometer with 5x5x10mm bars that were prepared by uniaxial pressing at 20 MPa followed by cold isostatic pressing at 200 MPa. They were heated inside the dilatometer furnace with a heating/cooling rate of 5°/min to 1680°C with a dwelling time of 10 hours. Additionally, 24mm diameter pellets were uniaxially pressed at 20MPa and sintered in air at 1100, 1200, 1300, 1400, 1500, and 1600°C with a dwell time of 2 hours and a heating/cooling rate of 5°C/min. One pellet was also sintered at 1700°C for 10 hours with a heating/cooling rate of 5°C/min in air. Another pellet was cold isostatically pressed (CIPed) at 200MPa in addition to being uniaxially pressed at 20 MPa and then sintered at 1700°C for 10 hours with a heating/cooling rate of 5°C/min in air. The density of each pellet was measured using the Archimedes method and the porosity was calculated using a theoretical density for the LSCMN powder of 6.40 g/cm³ [7].

Microstructure of both the powder and the fracture surfaces of the sintered pellets were analyzed using a Hitachi S-4700 FESEM with EDS attachment. Backscattered images were also captured of the polished and thermally etched surface of the CIPed sample. Grain size measurements were made using 200 measurements from the fracture surface micrographs, taking measurements in both the horizontal and vertical directions. Finally XRD patterns were obtained using a Scintag XDS 200 diffractometer with CuK_α radiation.

DISCUSSION

Figure 1 shows a micrograph of the LSCMN powder, the grain size distribution of the powder, and two XRD patterns of LSCMN ceramics. The morphology and particle size were estimated resulting in the average particle size of around 0.39 μm with some particles having diameters larger than 1.0 μm. The particles have well defined roundish shape yet clear facets could be distinguished by FESEM. The specific surface area of the powders was 2.01 m²/g as provided by Praxair. The XRD pattern of both LSCMN powders and sintered ceramics show typical reflections of orthorhombic *Pnma* perovskites (Fig. 1, ICDD card # 87-0015). Very weak peaks at 2θ = 38, 43, and 64° have been detected which are related to the small amount (about 1 wt %) of Mg_{0.6}Ni_{0.4}O secondary phase with a rock salt structure. One more peak at 2θ = 29° has been tentatively assigned to either Sr₃(CrO₄)₂ or Sr₄Cr₃O₉. Due to its very low intensity and overlap with the peaks of the major LSCMN perovskite phase it was not possible to make a more definite assignment of the existing phase.

The lattice parameters of the sintered LSCMN ceramics remained almost constant over the sintering temperatures with values of $a = 5.4715 \pm 0.0005 \text{ \AA}$, $b = 5.5134 \pm 0.0003 \text{ \AA}$, and $c = 7.745 \pm 0.001 \text{ \AA}$. These lattice parameters were used to determine the volume of the unit cell for the calculation of the theoretical density $\rho_{th} = 6.40 \text{ g/cm}^3$. As one can see from Figure 2 the porosity remains high (25-50%) for all sintering temperatures of the samples prepared using uniaxial pressing at 20 MPa. The measured raw density of the samples after uniaxial pressing before sintering was about 56%-58% therefore the particle packing density was not high. This led to the low final density of the sintered samples, even when sintering temperature was 1700°C and dwell time was 10 hours. The situation was dramatically improved when both uniaxial pressing at 20 MPa and cold isostatic pressing at 200 MPa were used for producing 73% dense

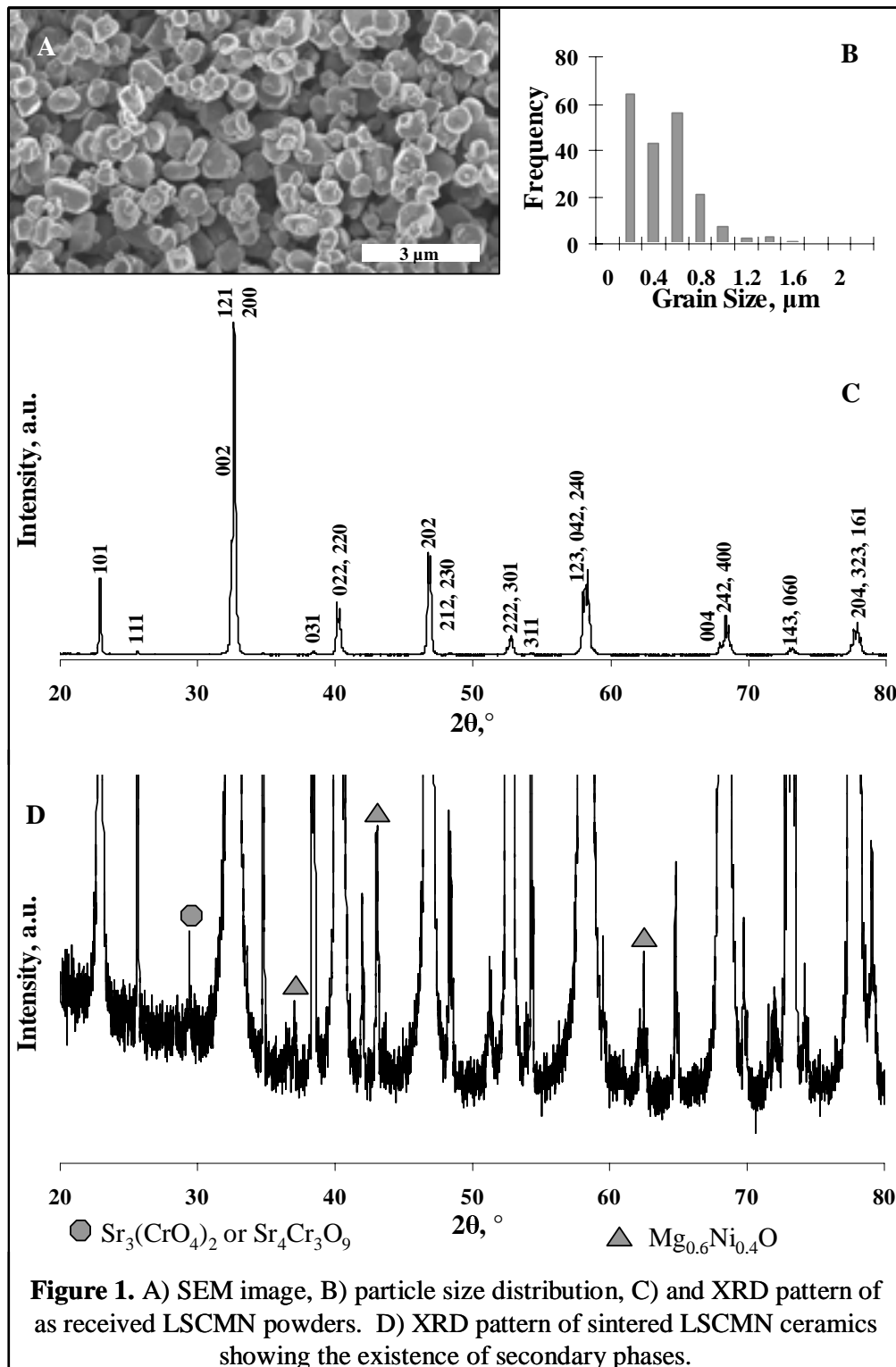


Figure 1. A) SEM image, B) particle size distribution, C) and XRD pattern of as received LSCMN powders. D) XRD pattern of sintered LSCMN ceramics showing the existence of secondary phases.

samples for sintering. After CIPing and sintering at 1700 $^\circ\text{C}$ for 10 hours the porosity of the sintered samples was about 5%, which means that the material has closed porosity and is gas tight. The measured average grain size of the LSCMN perovskite sintered at different temperatures is presented in Figure 2 along with the porosity of the samples. While the grain

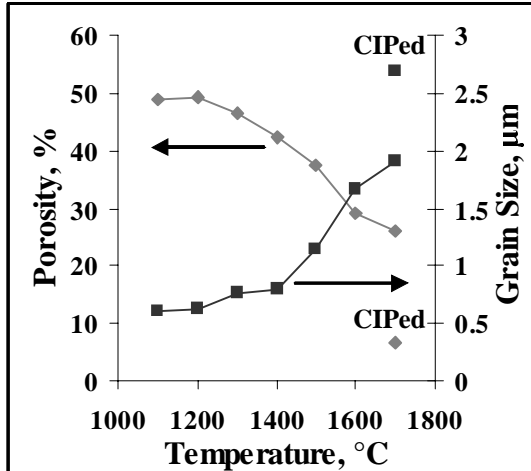


Figure 2. Grain size and porosity of the LSCMN as a function of sintering temperature.

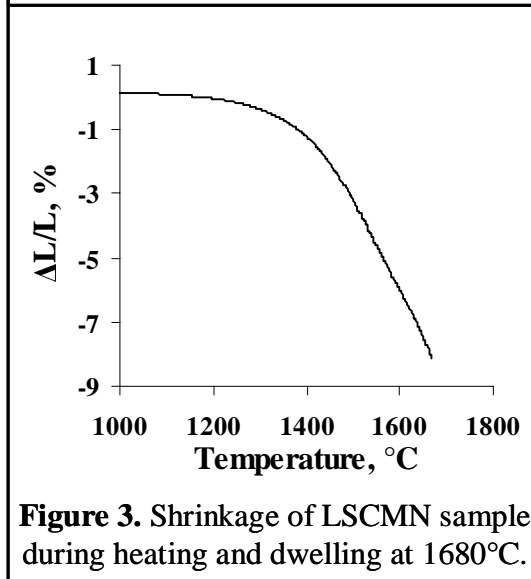


Figure 3. Shrinkage of LSCMN sample during heating and dwelling at 1680°C.

size remains almost the same as the particle size of the as received powders at 1100-1400°C sintering temperature, certain grain growth starts for sintering at 1500 to 1700°C.

Measurement of linear shrinkage during sintering at a constant heating rate is shown in Figure 3. It shows the appearance of only a single step broad sintering event, which indicates that this composition undergoes solid state sintering. Unlike multiple sintering steps reported in [8] for $(La_{0.7}Sr_{0.3})_xCrO_3$ ceramics, no evidence for occurrence of liquid state sintering was found for LSCMN composition. The rapid shrinkage of LSCMN occurs around 1500°C indicative of the beginning of the intensive solid state diffusion. Even at the 1680°C (the maximum temperature allowed by the dilatometer) the shrinkage did not end even after dwell time for 10 hours at this temperature. The high sintering temperature and high porosity indicates that LSCMN is difficult to sinter and CIP has to be used that the material can be sintered to the gas tight condition.

The backscattered SEM image of the LSCMN surface after CIPing and sintering at 1700°C for 10 hours, followed by polishing and thermal etching is shown in Figure 4 next to the secondary electron image of the same area. Two phases can be clearly distinguished, the major phase belonging to the perovskite phase, and the darker phase belonging to $Mg_{0.6}Ni_{0.4}O$ rock salt secondary phase, as it was confirmed by EDS (Fig. 4) In addition a third, lighter phase of low contrast can be found in the same image. EDS confirmed

this phase has higher Sr content than the main perovskite phase. The theoretical contrast between LSCMN and $Mg_{0.6}Ni_{0.4}O$ was calculated to be about 40%, while that between LSCMN and $Sr_3(CrO_4)_2$ or $Sr_4Cr_3O_9$ was found to be about 15%. Due to the radius of the excitation volume it was not possible to capture a scan of either secondary phase without some interference of the primary perovskite phase. The location of $Mg_{0.6}Ni_{0.4}O$ phase has been always found in the triple points, while Sr-rich secondary phase resided along the grain boundaries of the main perovskite grains.

An unusual 9-fold symmetry of the polyhedral surface termination steps has been found on the inner surfaces inside closed pores of $(La_{0.9}Sr_{0.1})_{0.95}Cr_{0.85}Mg_{0.1}Ni_{0.05}O_3$ perovskite pressureless sintered at 1700°C for 10 hours in air. An image of one such grain and a close up of a set of termination steps on another grain can be seen in Figure 5. The nanogons are usually formed at the corners of the grains in the (111) planes of the orthorhombic crystals. The formation of surface termination steps might be a result of the thermal etching of the free surface

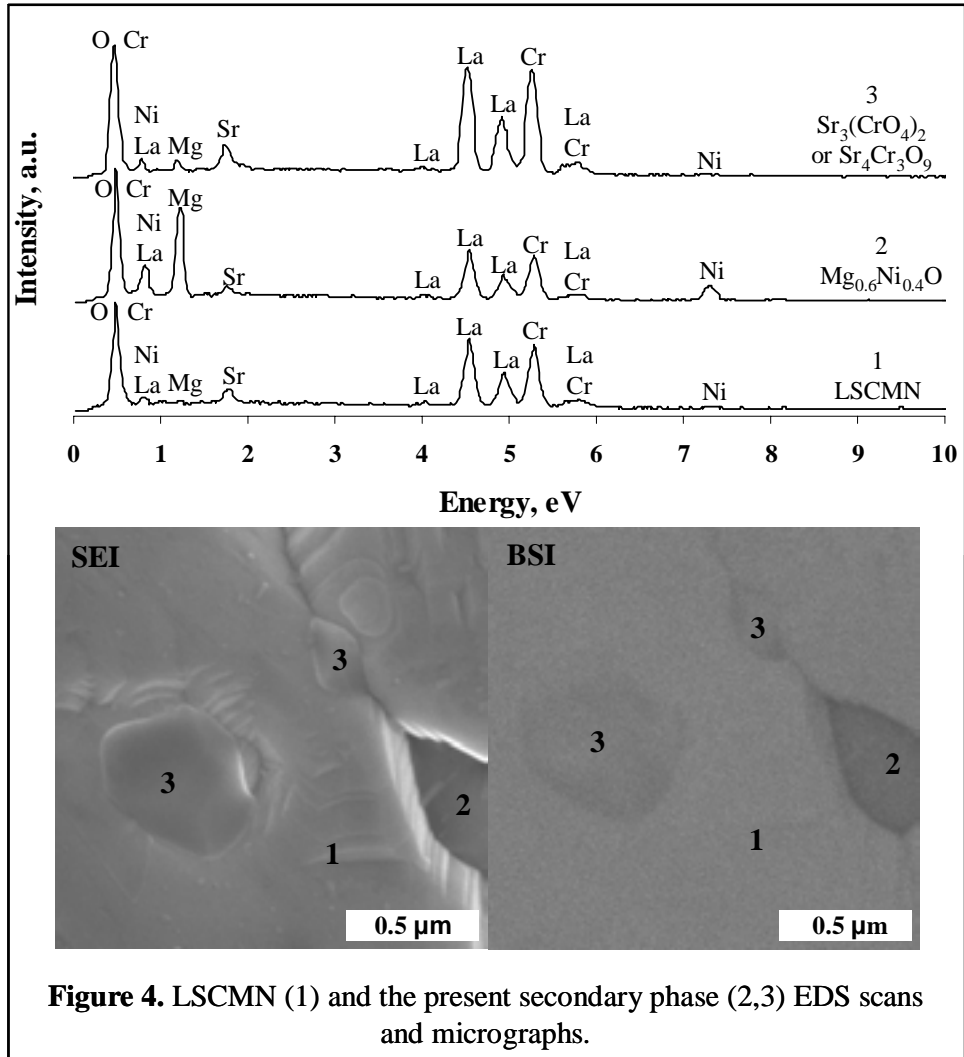


Figure 4. LSCMN (1) and the present secondary phase (2,3) EDS scans and micrographs.

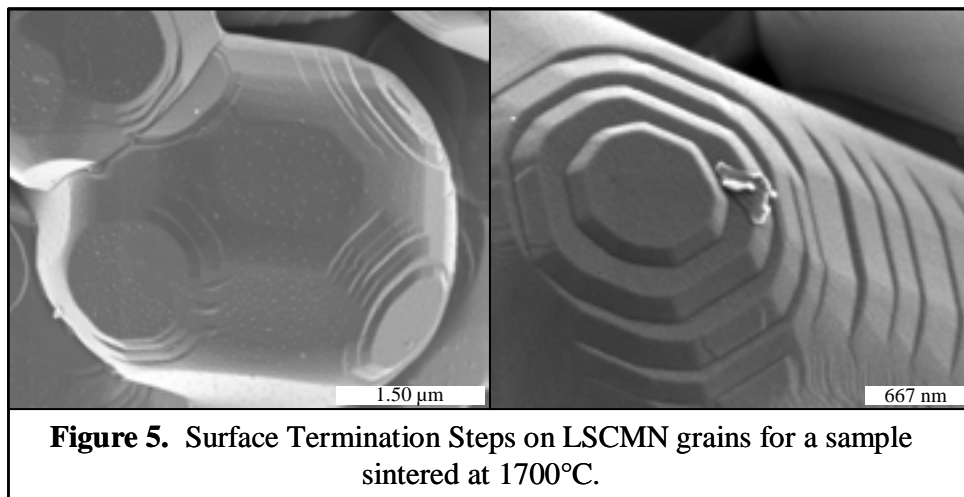


Figure 5. Surface Termination Steps on LSCMN grains for a sample sintered at 1700°C.

by gases trapped inside the pores during high temperature sintering. The steps also might appear as a result of the preferential grain growth kinetics during heating. Because orthorhombic perovskites should be heavily twinned, the steps might also be the sites where twins terminate at

the free surface. Such surface termination steps might contribute to the high catalytic activity of this orthorhombically distorted perovskite in the selective oxidation of hydrocarbons to produce synthesis gas.

CONCLUSIONS

The difficulties in sintering of $(\text{La}_{0.9}\text{Sr}_{0.1})_{0.95}\text{Cr}_{0.85}\text{Mg}_{0.1}\text{Ni}_{0.05}\text{O}_3$ perovskite ceramics were observed. This material cannot be sintered to high density in air, even at 1700°C with a dwell time of 10 hours, unless cold isostatic pressing is used to promote the preliminary densification of the raw pellet. Only after CIP it was possible to sinter LSCMN to 95% of theoretical density. The sintering of the LSCMN appears to be solid state, with no evidence of the liquid phase sintering that has been reported for other La-Cr-O compositions.

Secondary phases have been detected to exist both in the LSCMN powders and sintered samples. $\text{Mg}_{0.6}\text{Ni}_{0.4}\text{O}$ was detected by XRD, EDS, and backscattered imaging techniques as was an additional secondary phase that appears to be either $\text{Sr}_3(\text{CrO}_4)_2$ or $\text{Sr}_4\text{Cr}_3\text{O}_9$. The amounts of $\text{Mg}_{0.6}\text{Ni}_{0.4}\text{O}$ could be on the level of 3-5% and it means that the stoichiometry of the LSCMN is altered.

Surface termination steps have been found on the (111) planes of the LSCMN grains. The step edges might be perfect sites for numerous catalytic reactions, facilitating syngas production, or catalytic conversion of CO_2 by splitting the C-O bond into different value added products such as CO, CH_4 , methanol, or ethanol in the presence of steam.

ACKNOWLEDGMENTS

This research was supported by NSF DMR project 0502765 “NSF-Europe Materials Collaboration: Self-organized Nanostructured Thin Films for Catalysis in Perovskite Related Membrane Reactors” and NASA Grant NNC06GA17G: “State University System (SUS) of Florida Turbine Initiative: Advanced Turbines, Energy and Environment”.

REFERENCES

1. M. Mori, Y. Hiei, N. Sammes, *Solid State Ionics*, 135, 743-748, 2000.
2. J. Fergus, *Solid State Ionics*, 171, 1-15, 2004.
3. W. Shu, S. Deevi, *Materials Science and Engineering A*, 348, 227-243, 2003.
4. M. Mori, T. Yamamoto, T. Ichikawa, Y. Takeda, *Solid State Ionics*, 148, 93-101, 2002.
5. J. Carter, M. Nasrallah, H. Anderson, *Journal of Materials Science*, 31, 157-163, 1996.
6. N. Sakai, T. Kawada, H. Yokokawa, M. Dokiya, T. Iwata, *Journal of Materials Science*, 148, 93-101, 1990.
7. R. Rosten, M. Koski, E. Koppa, *Journal of Undergraduate Materials Research*, 2, 38-41, 2006.
8. S. Simners, J. Hardy, J. Stevenson, T. Armstrong, *Journal of Materials Science*, 34, 5721-5732, 1999.